Characterization of an Atmospheric Air Non-thermal Plasma Device in Relation to Ozone Production

Mooktzeng Lim, Kanesh Kumar Jayapalan, Ahmad Zulazlan Shah Zulkifli, Hamdan Hassan, Kailok Lai, and Oihoong Chin

Abstract—**An atmospheric air non-thermal plasma (NTP) device is characterized in relation to ozone production. The electron density, n_e, electron temperature, T_e and ozone concentration are measured for three dielectric barrier discharge (DBD) geometries, i.e., ten tubes of 10 mm outer diameter (OD), six tubes of 25 mm OD, and three tubes of 40 mm OD.n_e and T_e are deduced using optical emission spectroscopy via the line ratio method and the ozone concentrations are measured by using an ozone meter.n_e and ozone concentrations were the highest for the three tube-40 mm configuration, showing a correlation between the number of charged particles and ozone production.**

Index Terms—**Dielectric barrier discharge, environmental treatment, non-thermal plasma, ozone.**

I. INTRODUCTION

Non-thermal plasma (NTP) can be produced from dielectric barrier discharge (DBD) reactors, and can consist of either a single insulated electrode, two insulated electrodes or an insertion of a dielectric barrier in the space between both electrodes [1]. In atmospheric air, DBDs are able, via ionization, to produce chemically active species such as oxygen and hydroxyl radicals. These reactive species are useful in various applications, such as surface modification [2], [3], flue gas [4] and waste water treatment [5], assisting in combustion [6], [7] and for fuel synthesis [1]. The production of these reactive species is affected by the properties of the plasma, such as the electron density, n_e which is the number of electrons per unit volume produced by the discharge, and the electron temperature, T_e which gives the average energy of the electrons produced by the discharge. Hence, it is important to measure these two parameters. One of the important reactive species is ozone which is commonly produced in electrical discharges in air, and this work attempts to correlate the ozone production to n_e and T_e.

It is not suitable to use the conventional electrostatic Langmuir probe to measure the n_e and T_e for atmospheric pressure discharges. A non-invasive method is preferable, and the proposed method here is to use the optical emission spectra via the line ratio method; whereby, the measured intensity ratio of two electronic transitions of a discharge gas

element is used for the fitting and deduction of the aforementioned parameters. For a discharge in atmospheric air, the most commonly observed electronic transitional bands are from molecular nitrogen. Hence, the line ratio method can be applied by taking the intensity ratios of two vibro-rotational emission peaks from different nitrogen transitional band systems (e.g., second positive system and first positive system [8] or second positive system and first negative system [8]). These ratios are fitted to deduce the electron energy distribution function (EEDF) and electron drift velocity, v_d of the discharge electrons, which can be subsequently used to calculate n_e and T_e.

This study will characterize and compare differences in n_e and T_e for a NTP rig with different DBD geometries. As the rig would be used for environmental and combustion purposes, the ozone emissions are measured for the different geometries and are correlated to n_e and T_e.

II. METHODOLOGY

A. Experimental Set-up

Fig. 1(a) shows the schematic of the NTP rig in TNBR. The rig has an enveloping cylinder of inner diameter 110 mm that acts as the ground electrode. Silica tubes with a thickness of 2 mm are used as the dielectric barrier, and are held in place by a Teflon holder. The tubes are arranged in different geometries, consisting of i) ten tubes of 10 mm outer diameter OD each, ii) six tubes of 25 mm OD each, and iii) three tubes of 40 mm OD each, respectively. The inner surface of the silica tubes are lined with copper sheets that are connected to the high voltage supply. The shortest gap between silica tubes and the outer enveloping shell is 1 mm.

The input power into the NTP rig is supplied by a high voltage (HV) power supply (PVM 2000). The HV source includes a 2 kW VARIAC that controls the total power to the load, while the current is controlled by the duty cycle which provides the current pulses. The frequency is adjustable while a digital meter allows the operating frequency to be displayed. An individual analogue voltage meter reads the DC voltage of the power amplifier, and an oil filled transformer is also provided.

The discharge power from the NTP rig can be determined by connecting a capacitor in series (0.22 μF) to the electrode before grounding. The use of capacitor to determine the power dissipated in the DBD is a common practice in literature, since the voltage crossing the series capacitor (V_c) is proportional to the charge crossing the electrodes [9]. The capacitor is connected to an oscilloscope to determine the

voltage across the capacitor, V_c. From V_c, the charge accumulated in the capacitor can be determined via $Q=CV_c$. A Lissajous diagram (e.g., a plot of the charge Q versus voltage input V_{in}) can then be obtained. The discharge energy per cycle is determined by calculating the area under the curve. From the Lissajous diagram, the discharge power for different voltages, duty cycle, and electrode configurations was determined.

A Fluke 1750 clamp meter was used to measure the current and voltage drawn from the main supply (i.e., I_{main} and V_{main}, respectively) into the set-up for different voltage inputs, duty cycle, and electrode configurations. The different values of current input and voltage input will be used to develop the dimensionless correlation for estimating the discharge power.

The spectrometer is an AvaSpec-ULS2048 Starline model from Avantes that has four channels that are able to measure optical emissions in the ultraviolet (UV), visible (VIS) and near infrared (NIR) regions. Each channel covers wavelengths of 200 to 458, 455 to 683, 680 to 974 and 870 to 1030 nm respectively. The first two channels have UC, VC gratings while the final two channels have NC gratings. All channels are equipped with 2048 pixel CCD detectors, with a grating resolution of 1200 lines/mm and a slit width of 10 μm. All four channels of the spectrometer are connected to a 2 m four-furcated cable. The cable has a fibre optic probe at the end that is used to detect the optical emissions from the NTP rig. The AvaSoft spectrometer software is able to display and record the optical emissions in terms of spectral lines. From the experimental spectral lines, a mathematical model is used to estimate n_e and T_e.

An ozone meter (UV-106L Ozone Analyzer, Ozone Solutions) was used to measure the ambient concentration of ozone as a result of the ionization process from the NTP. The measurements were averaged over a period of 10 min.
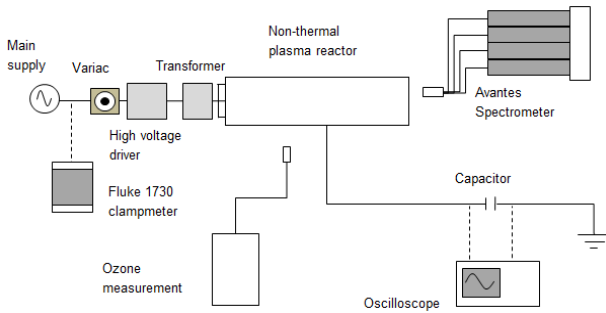

Fig.1. Schematic of non-thermal plasma test rig.

B. Modeling of Electron Density, n_e and Electron Temperature, T_e

A model has been developed to calculate the electron number density, n_e and electron temperature, T_e of the atmospheric NTP using the MATLAB software. The required input parameters of the model are the average current density, J_{ave} of the discharge and the spectral line intensity ratio.

For air plasmas at atmospheric pressure (with 78% Nitrogen, N_2 and 21% Oxygen, O_2 composition), the observed spectral lines (Fig. 2) are primarily from the N_2 molecular and N_2^+ ionic band transitions, known respectively as the second positive system (N_2 $C^3\Pi_u \rightarrow B^3\Pi_g$ or N_2 (C-B)) and the first

negative system (N_2^+ $B^2\Sigma_u^+ \rightarrow X^2\Sigma_g^+$ or N_2^+ (B-X)).

Taking the measured ratio of the most intense peak (v'-v''=(0-0)) of the second positive system at 337.1 nm and the first negative system at 391.4 nm (with consideration of the spectral efficiencies at each wavelength) it is possible to infer the electron velocity distribution by means of fitting with the following equation [10]-[13],

$$\frac{I_{N_2^+(B-X)}}{I_{N_2(C-B)}} = \frac{Q_{N_2^+(B-X)}}{Q_{N_2(C-B)}} \cdot \frac{\int f_v(E).E.\sigma_{exc}^{N_2^+(B-X)}dE}{\int f_v(E).E.\sigma_{exc}^{N_2(C-B)}dE}. \quad (1)$$
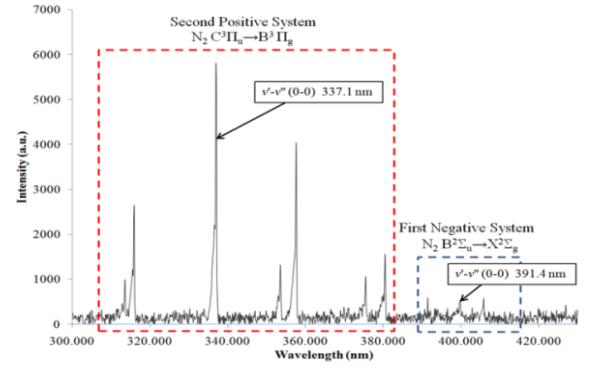

Fig. 2. Measured spectral lines from 300-450 nm for the discharge at 1.5 A for the 10 tube configuration.

Here, E is the energy of the electrons in eV, $f_v(E)$ is the electron velocity distribution function (EVDF) in $\text{eV}^{-3/2}$ and $\sigma_{exc}^{N_2(C-B)}$ and $\sigma_{exc}^{N_2^+(B-X)}$ are the electron impact excitation cross sections for the second positive and first negative system transitions in m^{-2} [14], respectively.

$Q_{N_2(C-B)}$ and $Q_{N_2^+(B-X)}$ are the rate coefficient ratios of the de-excitation and emission processes involved in the second positive and first negative systems respectively, and are given by:

$$Q_{N_2(C-B)} = \frac{A^{N_2(C-B)}}{A^{N_2(C-B)} + k_q^{N_2(C-B)}[N_2] + k_q^{N_2(C-B)}[O_2]}. \quad (2)$$

and

$$Q_{N_2^+(B-X)} = \frac{A^{N_2^+(B-X)}}{A^{N_2^+(B-X)} + k_q^{N_2^+(B-X)}[N_2] + k_q^{N_2^+(B-X)}[O_2]}, \quad (3)$$

$A^{N_2(C-B)}$ and $A^{N_2^+(B-X)}$ are the spontaneous emission (Einstein) coefficients for the second positive and first negative systems respectively in s^{-1} [15]; $k_q^{N_2(C-B)}$ and $k_q^{N_2^+(B-X)}$ are the molecular quenching rate coefficients for the second positive and first negative systems respectively in m^3s^{-1} [15]. $[N_2]$ and $[O_2]$ are the atmospheric nitrogen and oxygen densities in m^{-3}. $[N_2]$ and $[O_2]$ can be calculated by using the ideal gas law from percentage of composition, i.e.,

$$[N_2] = 0.78\frac{p}{k_B T_n} \approx 5.72\times10^{27}/T_n, \quad (4)$$

and

$$[O_2] = 0.21 \frac{p}{k_B T_n} \approx 1.54 \times 10^{27} / T_n , \qquad (5)$$

where, p is the atmospheric pressure in Pa, k_B is the Boltzmann constant in J K^{-1} and T_n is neutral gas temperature of the measured plasma in K. For certain NTP conditions, T_n is typically assumed to be close to room temperature, i.e., ~ 300 K. In the present work, however, T_n was calculated via simulation algorithm [16] to account for the effects of neutral gas heating on discharge parameters.

The EVDF, f_v is obtained by solving the Boltzmann equation for the electron collisional processes involved at the given conditions. A free Boltzmann solver program developed by Napartovich [17] was used for this purpose. The input parameters required for the program were the atmospheric gas composition, gas pressure and reduced electric field, *E/N* (in Td). The reduced electric field is the ratio between the electric field of the discharge with the total number of particles in the vicinity. The EVDFs were calculated for an E/N range of 50-1000 Td at 50 Td intervals. Each of the obtained EVDF distributions was used to calculate equation (1). The calculated theoretical ratios of $I_{N_2^+ (B-X)} / I_{N_2(C-B)}$ and fitted curve versus *E/N* are shown in Fig. 3The fitted curve in Fig. 3 is used to match the ratios measured from experimental data and find the corresponding value of *E/N*, i.e., the reduced electric field of the discharge.
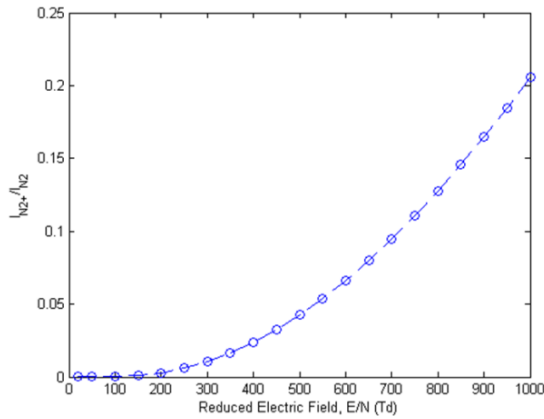

Fig. 3. Calculated theoretical ratios $I_{N_2^+ (B-X)} / I_{N_2(C-B)}$ versus reduced electric field, E/N (Td).

Electron temperature, T_e (eV) can be calculated from the EVDF by using the following equation,

$$T_e = \frac{2}{3} \int f_v(E) . E^{3/2} dE. \qquad (6)$$

For convenience, T_e is first obtained versus *E/N* at the same intervals as the theoretical ratios in Fig. 4; and is similarly fitted (Fig. 4). The fitted curve can next, be used to estimate T_e of the discharge by taking the earlier determined value of *E/N* from the measured line ratio.

Besides calculation of the EVDF, the Boltzmann solver by Napartovich is also able to calculate the electron drift velocities, v_d for each input value of *E/N*. v_d can be briefly described as the velocity of the electron flow under the influence of an electric field. The electron density, n_e can be

determined by v_d via,

$$n_e = \frac{J_{ave}}{e . v_d}. \qquad (7)$$

Here, e is the electron charge in C and J_{ave} is the average current density of the discharge given by,

$$J_{ave} = \frac{I_D}{S_D} , \qquad (8)$$

where, I_D is the measured discharge current and S_D is the surface area of the discharge. As with T_e in Fig. 4, the reciprocal term, $1/e.v_d$ is plotted versus *E/N* at the aforementioned intervals and fitted (Fig. 5). n_e of the discharge is then, estimated by multiplying J_{ave} with the matched value of $1/e.v_d$ determined from the previously obtained *E/N* of the discharge.
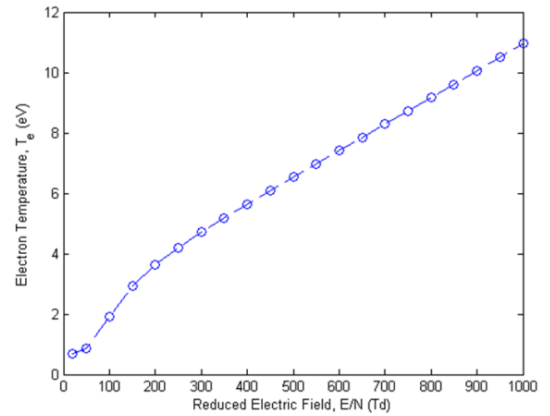

Fig. 4. Calculated theoretical electron temperature, T_e (eV) versus reduced electric field, *E/N* (Td).

III. RESULTS AND DISCUSSION

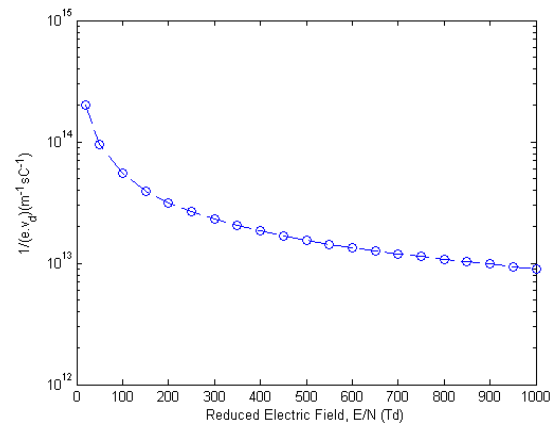#### A. Electron Density, n_e and Electron Temperature, T_e for Different Geometries

Fig. 5. Calculated reciprocal term $1/e.v_d$ (for calculation of n_e) versus reduced electric field, *E/N* (Td).

Fig. 6 shows the variation of n_e with different electrode diameters and discharge power. The calculated range of n_e were (0.67 - 0.75)$\times 10^{14}$ m^{-3}, (1.4 - 2.0) $\times 10^{14}$ m^{-3} and (1.9 -

2.7) $\times 10^{14}$ m^{-3} for the DBD geometries with the ten tubes of 10 mm diameter, six tubes of 25 mm diameter and three tubes of 40 mm diameter, respectively. n_e increases with the lower number of tubes due to the stronger electric fields generated (i.e., the same input power is divided across less tubes), allowing for increased ionization and collisional excitation of plasma electrons.
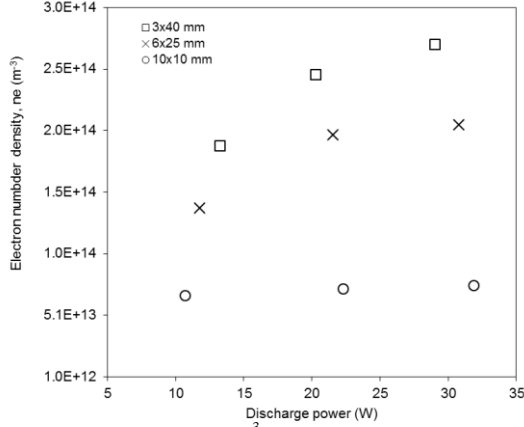

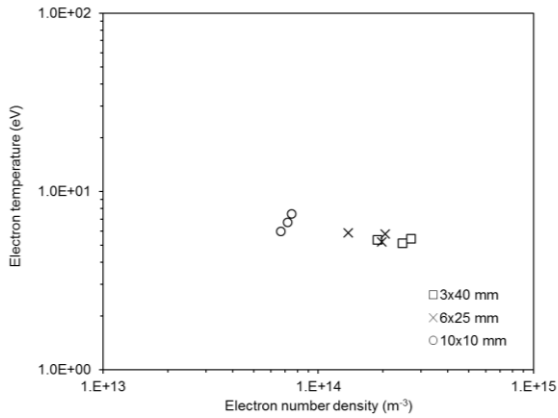Fig. 6. Electron density, n_e (m^{-3}) versus discharge power, P (W).

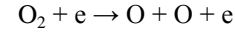Fig. 7. Variation of electron temperature, T_e (eV) with electron density, n_e (m^{-3}).

Fig. 7 shows the variation of T_e with the n_e. T_e decreases with increasing n_e; with the three tubes of 40 mm diameter geometry having the lowest temperature range of 5.1-5.4 eV. This can be attributed to Coulomb collisions between charged particles which becomes more significant as n_e increases [1].

B. Ozone Production for Different Geometries

The pathway of ozone production via electron impact ionization can be described as follows. Upon electron impact, inelastic collisions occur and modifies electronic structure of neutral species, creating excited species or ions [18]. In the case of inelastic collisions of electrons with nitrogen molecules, nitrogen is excited to ions that are in their ground state. When nitrogen ions, electrons and molecules collide, a three body reaction takes place to produce excited nitrogen molecules in the C-state ($C^3\Pi_u$), which is at a higher energy level (N$_2$ ($\upsilon>1$)) [19]-[21]. The excited nitrogen molecule is unstable, and is quenched to lower energy level states (B$^3\Pi_g$ and X$^2\Sigma_g$) after collisions with the oxygen molecules to generate atomic oxygen via two-step mechanism [20], [21]:

$$N_2 + e \rightarrow N_2 \, (\upsilon > 1) + e$$

$$N_2 \, (\upsilon>1)+O_2 \rightarrow N_2 + O + O$$
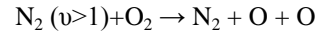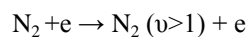
The decay to lower energy states emit an ultraviolet glow, of which spectra is similar to that shown in Fig. 2. In addition to the above reactions, atomic oxygen is produced by direct electron impact dissociation [21]:

$$O_2 + e \rightarrow O + O + e$$

Atomic O recombines with O$_2$ quickly to form ozone (O$_3$) based on the following reaction [4], [6], [22].

$$O_2 + O + M \rightarrow O_3 + M$$

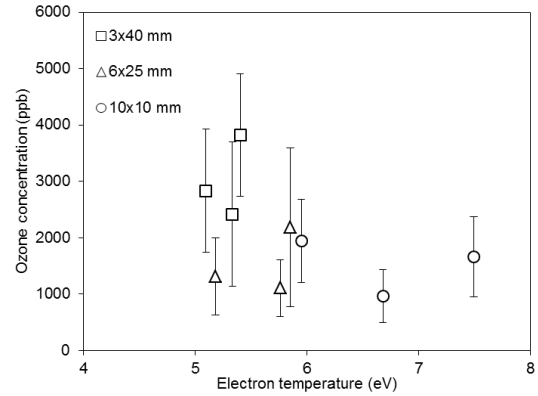where M is a third body collision partner.

Fig. 8. Variation of ozone concentration with electron temperature, T_e (eV).

As shown in Fig. 8, the amount of ozone from the three tubes of 40mm diameter electrode is the highest, showing that the energy via electron collisions has been used (i.e., lower T_e) to produce ozone. A higher production of charged particles, i.e. higher n_e, also indicates that more ozone will be produced (Fig. 9).
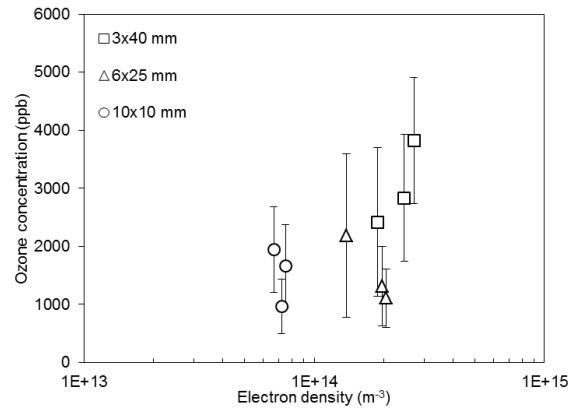

Fig. 9. Variation of ozone concentration with electron density, n_e (m^{-3}).

IV. CONCLUSION

The plasma characteristics of the TNBR NTP discharge has been determined by simulation using a line ratio code developed with MATLAB. Amongst the discharge parameters that were calculated include the reduced electric field, E/N, electron density, n_e and electron temperature, T_e. The obtained range of n_e were (0.67 - 0.75) $\times 10^{14}$ m^{-3}, (1.4 - 2.0) $\times 10^{14}$ m^{-3} and (1.9 - 2.7)$\times 10^{14}$ m^{-3} for the DBD geometries with ten tubes of 10 mm diameter, six tubes of 25 mm diameter and three tubes of 40 mm diameter, respectively. n_e is seen to increase with the lower number of tubes due to the

stronger electric fields generated, which allows for increased ionization and collisional excitation of plasma electrons. T_e, on the other hand, is seen to decrease with increasing n_e; the three tubes of 40 mm diameter geometry have the lowest temperature range of 5.1-5.4 eV. This is attributed to Coulomb collisions between charged particles which become more significant as n_e increases. The amount of ozone from the three tubes of 40 mm diameter electrode is the highest, showing that the energy has been used via electron collisions to produce ozone. A higher number of charged particles also indicate that more ozone will be produced.

REFERENCES

[1] H. Hao, B. S. Wu, J. Yang, Q. Guo, Y. Yang, and Y. W. Li, "Non-thermal plasma enhanced heavy oil upgrading," *Fuel*, vol. 149, 162, 2015.

[2] T. Acsente, M. D. Ionita, M. Teodorescu, V. Marascu, and G. Dinescu, "Surface modification of polymethylmethacrylate foils using an atmospheric pressure plasma jet in presence of water vapors," *Thin Solid Films*, 2015.

[3] M. Fabbri, M. Gigli, M. Costa, M. Govoni, P. Seri, N. Lotti, E. Giordano, A. Munari, R. Gamberini, B. Rimini, G. Neretti, A. Cristofolini, and C. A. Borghi, "The effect of plasma surface modification on the biodegradation rate and biocompatibility of a poly(butylene succinate)-based copolymer," *Polymer Degradation and Stability*, vol. 121, p. 271, 2015.

[4] M. Babaie, P. Davari, P. Talebizadeh, F. Zare, H. Rahimzadeh, Z. Ristovski, and R. Brown, "Performance evaluation of non-thermal plasma on particulate matter, ozone and CO_2 correlation for diesel exhaust emission reduction," *Chemical Engineering Journal*, vol. 276, p. 240, 2015.

[5] B. Jiang, J. Zheng, S. Qiu, M. Wu, Q. Zhang, Z. Yan, and Q. Xue, "Review on electrical discharge plasma technology for wastewater remediation," *Chemical Engineering Journal*, vol. 236, p. 348, 2014.

[6] T. Ombrello, S. H. Won, Y. Ju, and S. Williams, "Flame propagation enhancement by plasma excitation of oxygen. Part I: Effects of O3," *Combustion and Flame*, vol. 157, 1906, 2010.

[7] T. Ombrello, S. H. Won, Y. Ju, and S. Williams, "Flame propagation enhancement by plasma excitation of oxygen. Part II: Effects of O2(a1Δg)," *Combustion and Flame*, vol. 157, 2010.

[8] J. H. Kim, Y. H. Choi, and Y. S. Hwang, "Electron density and temperature measurement method by using emission spectroscopy in atmospheric pressure nonequilibrium nitrogen plasmas," *Physics of Plasmas*, vol. 13, 2006.

[9] J. Kriegseis, B. Möller, S. Grundmann, and C. Tropea, "Capacitance and power consumption quantification of dielectric barrier discharge (DBD) plasma actuators," *Journal of Electrostatics*, vol. 69, 2011.

[10] S. Kühn, N. Bibinov, R. Gesche, and P. Awakowicz. "Non-thermal atmospheric pressure HF plasma source: Generation of nitric oxide and ozone for bio-medical applications," *Plasma Sources Science and Technology*, vol. 19, 2010.

[11] P. Rajasekaran, "Atmospheric-pressure Dielectric barrier discharge (DBD) in air: Plasma characterization for skin therapy," PhD dissertation, Institute for Electrical Engineering and Plasma Technology, Ruhr-Universität Bochum, Bochum, Germany, 2011.

[12] P. Rajasekaran, N. Bibinov, and P. Awakowicz, "Quantitative characterization of a dielectric barrier discharge in air applying non-calibrated spectrometer, current measurement and numerical simulation," *Measurement Science and Technology*, vol. 23, 2012.

[13] P. Rajasekaran, P. Mertmann, N. Bibinov, D. Wandke, W. Viöl, and P. Awakowicz, "DBD plasma source operated in single-filamentary mode for therapeutic use in dermatology," *Journal of Physics D: Applied Physics*, vol. 42, 2009.

[14] Y. Itikawa, "Cross sections for electron collisions with nitrogen molecules," *Journal of Physical and Chemical Reference Data*, vol. 35, 2006.

[15] S. V. Pancheshnyi, S. M. Starikovskaia, and A. Y. Starikovskii, "Collisional deactivation of N2(C 3Πu, v=0, 1, 2, 3) states by N2, O2, H2 and H2O molecules," *Chemical Physics*, vol. 262, 2000.

[16] K. K. Jayapalan and O. H. Chin, "Effect of neutral gas heating on the wave magnetic fields of a low pressure 13.56 MHz planar coil inductively coupled argon discharge," *Physics of Plasmas*, vol. 21, 2014.

[17] N. A. Dyatko, I. V. Kochetov, A. P. Napartovich, and A. G. Sukharev, *Institute for Innovation and Fusion Research*, Troizk, Moscow Region, Russia,1991.

[18] C. Tendero, C. Tixier, P. Tristant, J. Desmaison, and P. Leprince, "Atmospheric pressure plasmas: A review," *Spectrochimica Acta Part B: Atomic Spectroscopy*, vol. 61, 2006.

[19] B. F. W. Vermeltfoort, "Experimental investigation of plasma assisted combustion using a low swirl burner," MSc. thesis, Department of Mechanical Engineering, Eindhoven University of Technology, Eindhoven, Netherlands., 2010.

[20] A. Starikovskiy and N. Aleksandrov, "Plasma-assisted ignition and combustion," *Progress in Energy and Combustion Science*, vol. 39, 2013.

[21] H. Hu, Q. Song, Y. Xu, G. Li, and C. Nie, "Non-equilibrium plasma assisted combustion of low heating value fuels," *Journal of Thermal Science*, vol. 22, 2013.

[22] Y. Ju and W. Sun, "Plasma assisted combustion: Dynamics and chemistry," *Progress in Energy and Combustion Science*, vol. 48, 2015.

Mooktzeng Lim obtained his Ph.D from University of Canterbury, New Zealand in chemical and process engineering, with focus on hydrodynamics of dual fluidized beds. He obtained his bachelors degree from Universiti Tenaga Nasional in mechanical engineering, while his MSc. studies was with Universiti Sains Malaysia, focusing on a 600 kW_{th} bubbling fluidized bed biomass gasifier. He has several postdoctoral stints with University of Canterbury, Uni. Teknologi PETRONAS, and University of Newcastle upon Tyne. Through these experiences, his research has expanded into dual fluidized bed gasification, entrained flow gasification, biodiesel production, and particulate emissions from biomass combustion. Mooktzeng has also worked as a mechanical engineer for three years and was involved in the maintenance department, and is now a Chartered Engineer with the Institutions of Mechanical Engineers (IMechE). He is registered as an Independent mentor with IMechE.

Mooktzeng is currently a principal researcher in the Fuels and Combustion Group of TNB Research Sdn. Bhd. working on non-thermal plasma devices, flame diagnostics, coal and biomass combustion.

Kanesh Kumar Jayapalan received his B.Sc. in applied physics and the PhD in plasma physics from the University of Malaya, Malaysia in 2006 and 2015, respectively. He is presently a post doctoral researcher attached with the Plasma Technology Research Center, Physics Dept., Uni. Malaya, working on simulation of atmospheric non-thermal plasma devices. His research interests include inductively coupled plasmas, atmospheric plasma jets and microdischarges.